

Supplementary material of

Vibrational and elastic properties of As_4O_6 and $\text{As}_4\text{O}_6 \cdot 2\text{He}$ at high pressures: study of dynamical and mechanical stability

V.P. Cuenca-Gotor,¹ O. Gomis,^{2,a)} J.A. Sans,¹ F. J. Manjón,¹
P. Rodríguez-Hernández,³ and A. Muñoz³

¹ Instituto de Diseño para la Fabricación y Producción Automatizada, MALTA Consolider Team, Universitat Politècnica de València, 46022 València, Spain

² Centro de Tecnologías Físicas: Acústica, Materiales y Astrofísica, MALTA Consolider Team, Universitat Politècnica de València, 46022 València, Spain

³ Departamento de Física, Instituto de Materiales y Nanotecnología, MALTA Consolider Team, Universidad de La Laguna, 38205 Tenerife, Spain

a) Author to whom correspondence should be addressed. Electronic mail: osgohi@fis.upv.es

A. Lattice dynamics

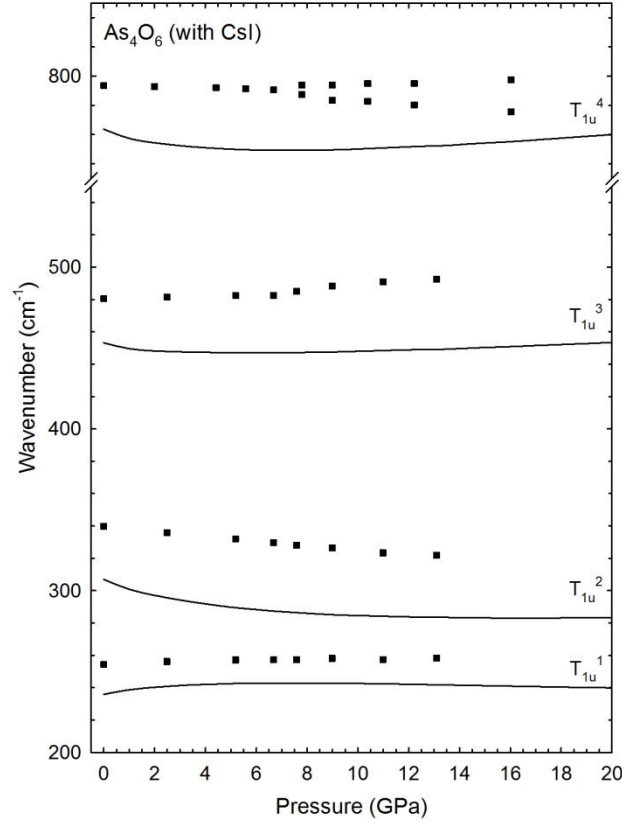


Figure S1. Experimental and theoretical pressure dependence of the IR-active modes in As_4O_6 . Experimental data measured using CsI as a PTM are taken from Ref. S1.

Table SI. Theoretical and experimental zero-pressure frequencies and pressure coefficients of IR-active modes in As_4O_6 at 0 GPa. Experimental data are taken from Ref. S1.

Mode (Sym)	Ab initio calculations		Experimental	
	ω_0 (cm^{-1})	$\frac{\partial \omega}{\partial P}$ ($\frac{\text{cm}^{-1}}{\text{GPa}}$)	ω_0 (cm^{-1})	$\frac{\partial \omega}{\partial P}$ ($\frac{\text{cm}^{-1}}{\text{GPa}}$)
T_{1u}^1 (IR)	236.0	2.7	254.5	0.8
T_{1u}^2 (IR)	306.7	-5.7	339.8	-1.5
T_{1u}^3 (IR)	453.1	-3.8	480.4	0.1
T_{1u}^4 (IR)	763.5	-6.6	793.4	-0.2

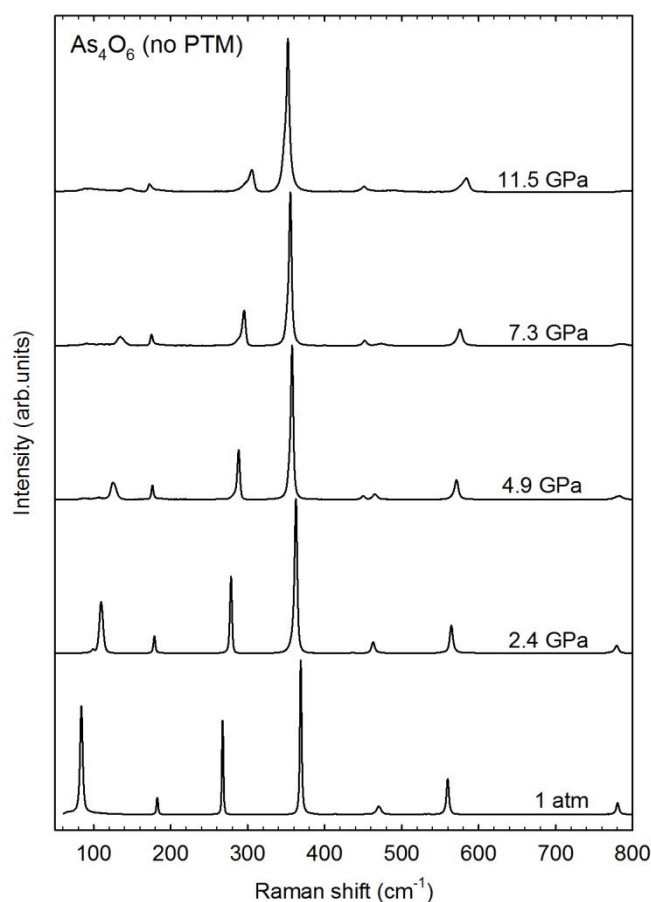


Figure S2. Raman scattering spectra of arsenolite at selected pressures without any PTM. Raman spectra are vertically shifted for the sake of clarity.

A progressive shift of the Raman-active mode frequencies of all peaks of the cubic structure with increasing pressure is observed in As_4O_6 compressed without any PTM. Absence of new peaks at high pressure clearly indicates that no phase transition occurs along the pressure range studied. Many Raman modes undergo a progressive asymmetric broadening with increasing pressure. This broadening is likely caused by the increase of intermolecular interactions; i.e., the increase of interactions among As_4O_6 cages, which finally results in the onset of PIA above 15 GPa.

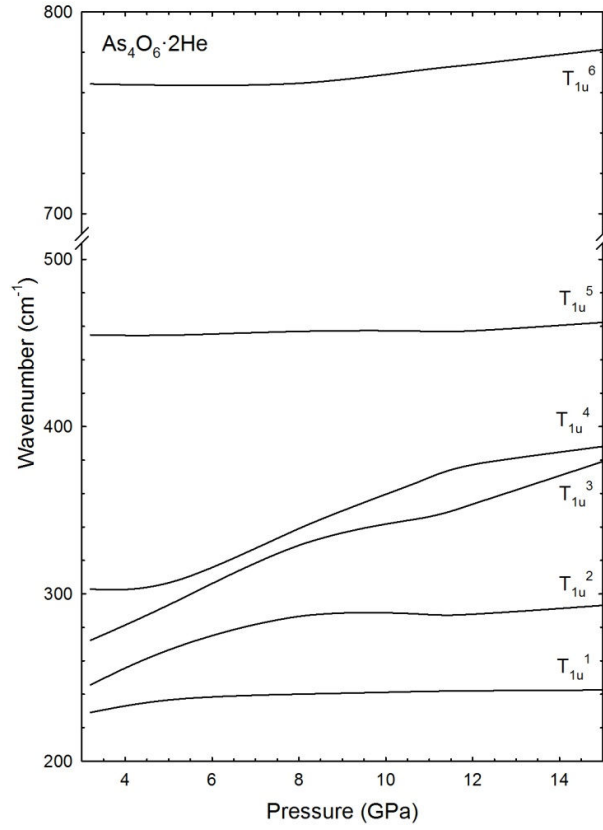


Figure S3. Theoretical pressure dependence of the IR-active modes in $\text{As}_4\text{O}_6 \cdot 2\text{He}$.

There are two additional IR-active modes in $\text{As}_4\text{O}_6 \cdot 2\text{He}$ than in As_4O_6 . The two extra modes are located between the two lowermost IR-active modes of As_4O_6 and have a much larger pressure coefficient than IR-active modes of As_4O_6 thus leading to anticrossings with the mode above 300 cm^{-1} .

Table SII. Theoretical frequencies and pressure coefficients of IR-active modes in $\text{As}_4\text{O}_6 \cdot 2\text{He}$ at 3 GPa.

Mode (Sym)	Ab initio calculations	
	ω_0 (cm^{-1})	$\frac{\partial \omega}{\partial P}$ ($\frac{\text{cm}^{-1}}{\text{GPa}}$)
T_{1u}^1	230.0	3.3
T_{1u}^2	247.5	11.2
T_{1u}^3	271.6	12.5
T_{1u}^4	300.3	0.3
T_{1u}^5	455.1	-0.7
T_{1u}^6	763.8	-1.1

B. Thermodynamic properties

The Debye temperature is a fundamental parameter that correlates with many physical properties of solids, such as specific heat, elastic constants, and melting temperature. One of the standard methods to calculate the Debye temperature, θ_D , is from elastic constant data using the semi-empirical formula [S2]:

$$\theta_D = \frac{h}{k_B} \left[\frac{3n}{4\pi} \left(\frac{N_A \rho}{M} \right) \right]^{1/3} v_m$$

where h is the Planck's constant, k_B is the Boltzmann's constant, n is the number of atoms in the molecule, N_A is the Avogadro's number, ρ is the density, M is the molecular weight, and v_m is the averaged sound velocity. As reported in **Table SIII**, the values of θ_D at 0 GPa using the Hill approximation are 196.2 K (222.7 K) in As_4O_6 ($\text{As}_4\text{O}_6 \cdot 2\text{He}$). We note that the Debye temperature in $\text{As}_4\text{O}_6 \cdot 2\text{He}$ is slightly greater than that of As_4O_6 . **Figure S4(a)** reports the evolution with pressure of the Debye temperature, θ_D , for both oxides. It is observed that θ_D follows a similar dependence than v_m with increasing pressure; i.e., increases at low pressures in both oxides and decreases above 8 GPa in As_4O_6 while it increases in $\text{As}_4\text{O}_6 \cdot 2\text{He}$ at least up to 35 GPa.

The thermal conductivity is the property of a material that indicates its ability to conduct heat. In order to estimate the theoretical minimum of the thermal conductivity, we have used the following expression [S3]:

$$\kappa_{\min} = k_B v_m \left(\frac{M}{n \rho N_A} \right)^{-2/3}$$

The values of κ_{\min} in As_4O_6 ($\text{As}_4\text{O}_6 \cdot 2\text{He}$) at 0 GPa using the Hill approximation are 0.36 (0.42) $\text{W m}^{-1} \text{K}^{-1}$ (see **Table SIII**). Therefore, both oxides are low κ materials [S4]. **Figure S4(b)** reports the evolution with pressure of the minimum thermal conductivity, κ_{\min} , for both oxides. As in the case of θ_D , κ_{\min} first increases with pressure and latter it decreases with pressure because of the decreasing of v_m with pressure for As_4O_6 , while κ_{\min} increases with pressure up to 35 GPa in $\text{As}_4\text{O}_6 \cdot 2\text{He}$. On the other hand, if we use the simplified formula for κ_{\min} that considers $v_m = 0.87 \sqrt{E/\rho}$ [S3], the decreasing of κ_{\min} with pressure in As_4O_6 can be explained by the decreasing of the tensile stiffness of As_4O_6 as pressure increases above 9 GPa.

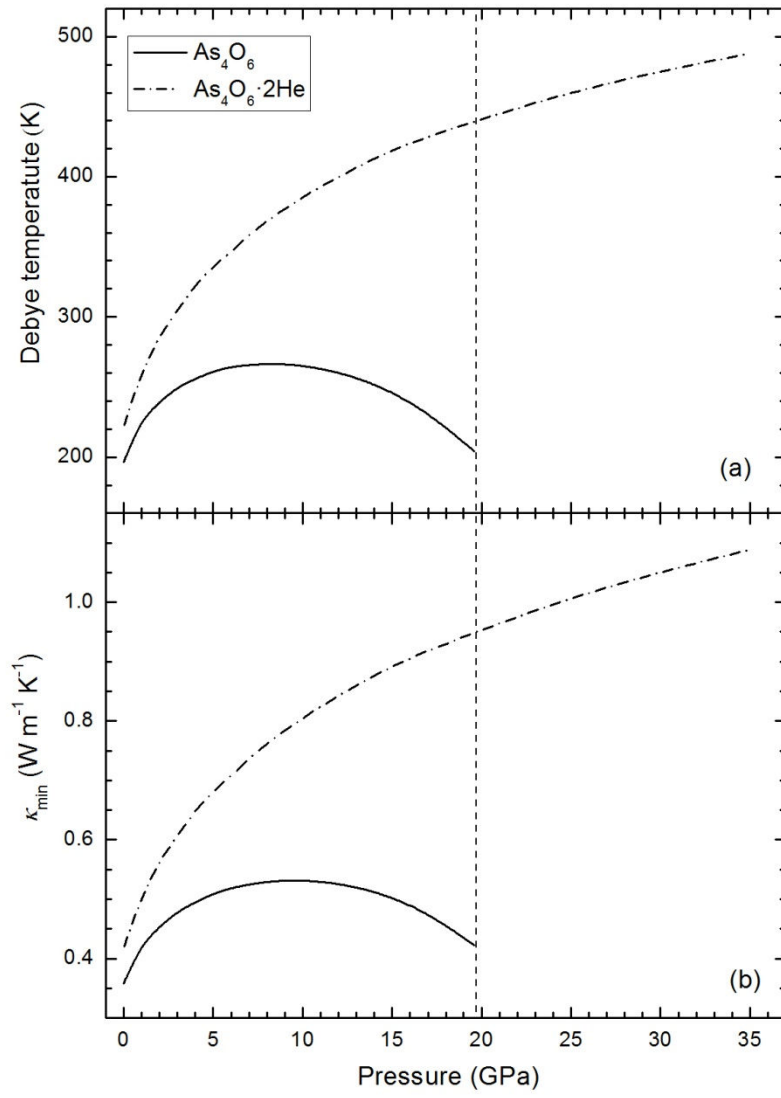


Figure S4. Evolution with pressure of the theoretical Debye temperature (a) and theoretical minimum thermal conductivity, κ_{\min} , (b) in As_4O_6 and $\text{As}_4\text{O}_6 \cdot 2\text{He}$.

Table SIII. Debye temperature (θ_D in K), and minimum thermal conductivity (κ_{\min} in $\text{W m}^{-1} \text{K}^{-1}$) in As_4O_6 and $\text{As}_4\text{O}_6 \cdot 2\text{He}$ at 0 GPa. Data are given in the Hill approximation.

	As_4O_6	$\text{As}_4\text{O}_6 \cdot 2\text{He}$
θ_D	196.2	222.7
κ_{\min}	0.36	0.42

References

- [S1] A. Grzechnik, J. Solid State Chem. 144, 416 (1999).
- [S2] O. L. Anderson, J. Phys. Chem. Solids 24, 909-917 (1963).
- [S3] D. R. Clarke, Surf. Coat. Technol. 163, 67-74 (2003).
- [S4] C. G. Levi, Curr. Opin. Solid State Matter. Sci. 8, 77-91 (2004).